Potent laminin-inspired antioxidant regenerative dressing accelerates wound healing in diabetes

Yunxiao Zhu[a], Zdravka Cankova[a], Marta Iwanaszko[b], Sheridan Lichtor[c], Milan Mrksich[a,d,e,1], and Guillermo A. Ameer[a,e,f,1]

[a]Department of Biomedical Engineering, Northwestern University, Evanston, IL 60208; [b]Department of Preventive Medicine, Feinberg School of Medicine, Northwestern University, Chicago, IL 60611; [c]Department of Chemical and Biological Engineering, Northwestern University, Evanston, IL 60208; [d]Department of Chemistry, Northwestern University, Evanston, IL 60208; [e]Center for Advanced Regenerative Engineering, Northwestern University, Evanston, IL 60208; and [f]Department of Surgery, Feinberg School of Medicine, Northwestern University, Chicago, IL 60611

The successful treatment of chronic dermal wounds, such as diabetic foot ulcers (DFU), depends on the development of safe, effective, and affordable regenerative tools that the surgeon can rely on to promote wound closure. Although promising, strategies that involve cell-based therapies and the local release of exogenous growth factors are costly, require very long development times, and result in modest improvements in patient outcome. We describe the development of an antioxidant shape-conforming regenerative wound dressing that uses the laminin-derived dodecapeptide A5G81 as a potent tethered cell adhesion-, proliferation-, and haptokinesis-inducing ligand to locally promote wound closure. A5G81 immobilized within a thermoresponsive citrate-based hydrogel facilitates integrin-mediated spreading, migration, and proliferation of dermal and epidermal cells, resulting in faster tissue regeneration in diabetic wounds. This peptide-hydrogel system represents a paradigm shift in dermoconductive and dermoinductive strategies for treating DFU without the need for soluble biological or pharmacological factors.

wound healing | regenerative biomaterials | citric acid | diabetic foot ulcers | laminin

Diabetes is the leading cause of nontraumatic limb amputations in the world, and the number of people with diabetes is rapidly growing, particularly in developing countries (1, 2). A major contributing factor to these amputations is the development of foot ulcers, which is experienced by as many as 25% of diabetics and can lead to frequent hospitalizations due to chronic nonhealing wounds (3). Although the field of wound care management is well established, the effective treatment of chronic diabetic foot ulcers remains a challenge due to oxidative stress, impaired angiogenesis, and exacerbated inflammation in the wound bed (4).

To address these issues, research and development efforts have recently focused on the local release of drugs or proteins, microRNA, DNA, and the use of autologous or allogeneic cells to fabricate skin tissue equivalents (4–6). Although promising, products that result from these strategies face substantial regulatory hurdles that complicate and delay translation to the clinic, due to their classification as drugs, biologics, or combination products by the Food and Drug Administration (FDA). Even when approved for human use, narrow indications of use, high costs, and negative side effects that are often observed when a product is introduced into the general population limit widespread adoption among physicians and patients. This was the case with Regranex (becalpermin), a gel based on a recombinant platelet-derived growth factor that was found to increase the risk of cancer with overuse and led to a warning label requirement by the FDA (7, 8). Other challenges with strategies that use drugs or biologics to treat nonhealing diabetic foot ulcers include limited product shelf life, which reduces widespread distribution to patients, an incomplete understanding of the mechanism of action, and untoward systemic side effects (9, 10).

Herein, we describe a biomaterials-based approach, that does not involve the inclusion or release of drugs, proteins, or cells, to create a shape-conforming regenerative wound dressing that significantly improves the healing rate of diabetic wounds. This approach is based on functional motifs from laminin and an understanding that the activation of the integrin α3β1 is essential for dermal fibroblast migration and epidermis keratinocyte reepithelialization of the wound (11–13). In this context, we selected a 12-amino acid sequence in the α5 globular domain of laminin referred to as A5G81 (14). This sequence has been reported to be a cell adhesion domain in laminin that interacts specifically with the integrins α3β1 and α6β1 (15). This adhesion mechanism is different from that of the commonly used fibronectin-derived arginyl-glycyl-aspartic acid (RGD) adhesion sequence, which is known to interact with a variety of integrin receptors including all five αV-containing integrins as well as α5β1, α8β1, and αIIbβ3 (16). We hypothesized that conjugating the laminin-derived peptide A5G81 to a thermoresponsive antioxidant bioresorbable citrate-based macromolecule would enable the formation of a self-assembling hydrogel that enhances the adhesion, migration, and proliferation of dermal cells, leading to improved wound-closure rates.

The antioxidant macromolecule poly(polyethylene glycol cocitric acid-co-N-isopropylacrylamide) (PPCN) undergoes a rapid and reversible phase transition from liquid to solid at physiologically relevant temperatures to form a hydrogel that conforms to the wound (17). PPCN was functionalized at the same molar concentration with either A5G81 or RGD to provide biological cues to dermal cells. Incorporation of the A5G81 peptide

Significance

The clinical management of nonhealing ulcers requires advanced materials that improve wound-closure rates without relying on the release of drugs or other growth factors that could potentially lead to concerns regarding systemic deleterious side effects. We report the synthesis, characterization, and performance of a biodegradable antioxidant shape-conforming regenerative dressing that exploits α3β1 and α6β1 integrin-binding interactions to promote dermal tissue regeneration. A laminin-derived peptide grafted onto a thermoresponsive citrate-based macromolecular scaffold facilitates the adhesion and spreading of skin cells throughout the hydrogel and also significantly increases cell proliferation and migration in an integrin-dependent manner. We use a splinted excisional wound diabetic mouse model to demonstrate that application of this thermoresponsive regenerative dressing significantly accelerates wound closure in vivo.

significantly improved the adhesion, spreading, proliferation, and migration of human dermal and epidermal cells in the PPCN network in an integrin-dependent manner. This work reports a tethered laminin-derived peptide that is capable of enhancing all of these cellular processes, which are critical to improving wound healing. Upon validation in a large animal model, PPCN-A5G81 may have a faster path to market as a tool to promote healing in diabetic foot ulcers.

Results

The Complete A5G81 Dodecapeptide Sequence Is Necessary to Promote the Adhesion and Haptokinesis of Human Epithelial Keratinocytes. The cost-effective fabrication and scale-up of a peptide-based regenerative dressing requires the identification of the minimum peptide length and amino acid sequence that is necessary to support the adhesion of dermal fibroblasts and epithelial keratinocytes. To achieve these tasks, we performed amino acid truncation and alanine substitution of individual residues of A5G81 using thiol-terminated peptides that were conjugated to self-assembled monolayers (SAMs) of maleimide-terminated dioctadecyl disulfide on gold-coated glass coverslips (all peptides at 1 mol% surface density) (Fig. 1) (18). Both of these modifications resulted in a significant loss of cell adhesion to the immobilized peptide, confirming that the complete A5G81 dodecapeptide and original sequence are necessary for cell adhesion (Fig. 1 B and C). We used the A5G81 truncated sequence WHRVSVC, which is a peptide we found during the truncation study that supports minimum cell adhesion and is referred to as inactive, as a control peptide for all subsequent experiments. Both the immobilized A5G81 and RGD peptides were biologically active, as they induced focal adhesion kinase expression, although there was a significantly larger number of adhered cells on the A5G81-presenting surfaces relative to RGD-presenting surfaces (*SI Appendix*, Fig. S1). In addition to cell adhesion, the

migration of adherent human epithelial keratinocytes (HEKas) on SAMs that display the various peptides, also at the same surface density, was evaluated using live cell time-lapse imaging. Individual cell tracking revealed that the immobilized A5G81 peptide significantly increased the average migration distance of HEKas (Fig. 2A) and effected a twofold increase in their average migration rate (Fig. 2B and *SI Appendix*, Fig. S2). In addition, the adherent cells were significantly more mobile on the A5G81-presenting surface, demonstrating this peptide's superior haptokinetic properties (Fig. 2 and *SI Appendix*, Fig. S2). Consistent with the adhesion study, we found that very few cells adhered to surfaces displaying the inactive peptides, and the migration of these cells was very limited (Fig. 2 and *SI Appendix*, Fig. S1).

To further determine what other cellular processes are triggered by the cell–peptide interaction, we performed a global gene expression analysis. We compared the transcriptional activities of HEKas cultured on the A5G81-presenting monolayers to those grown on the RGD-presenting monolayers, both at the same surface peptide density of 1% that has been shown to reduce nonspecific interactions (19). Consistent expression readouts were obtained from triplicate experiments within each group, confirming the reliability of the peptide-SAM surface functionalization method. To generate an integrated view of the effects of A5G81 on HEKa, we performed pathway analysis using GOrilla gene ontology enrichment analysis (20). This analysis provides gene clustering information based on known functional interactions such as protein–protein interactions of gene regulation interactions and demonstrates the interconnectivity between genes. Among all of the cellular networks, three cell surface receptors and cell proliferation related networks were identified with a *P* value lower than 0.05 and were merged together to generate an integrated picture of relevant relationships among the pathways (Fig. 2 C and D). Data analysis shows that, during the 12-h incubation time, significant gene expression changes occur in genes involved in cytokine-mediated signaling pathway [gene ontology (GO): 0019221], cell surface receptor signaling pathway (GO: 0007166), and the negative regulation of growth pathway (GO: 45926). The first two pathways, which include keratinocyte development markers such as KRT7 and KRT19, were mostly upregulated in cells grown on A5G81 surfaces. These results are consistent with the elevated cell matrix interactions and cellular activity levels triggered by A5G81. Genes associated with negative regulation of cell growth were found to be up-regulated in cells grown on surfaces displaying RGD and not on surfaces displaying A5G81. Additionally, migration-associated genes including ICAM1, OAS2, and IFIT2 were up-regulated in the A5G81 group (21, 22). These results are consistent with the increased cell proliferation and migration rates observed in the A5G81 group.

The Biological Functions of A5G81 Can Be Harnessed Within a 3D Thermoresponsive Antioxidant Macromolecular Network. We synthesized an A5G81-presenting thermoresponsive and antioxidant macromolecular network (A5G81-PPCN) by conjugating the cysteine-terminated A5G81 peptide to maleimide-functionalized PPCN (Fig. 3A). With a similar strategy, we also synthesized RGD-presenting PPCN (RGD-PPCN) and inactive peptide-presenting PPCN (inactive-PPCN) as per MALDI data (Fig. 3B and *SI Appendix*, Fig. S3). The final concentration of the peptide motif in the peptide-PPCN was verified to be 1 mM for all groups throughout the study (*SI Appendix*, Fig. S4). Tethering the peptide to the macromolecule lowered PPCN's intrinsic lower critical solution temperature (LCST) by a few degrees (24 °C for AG581-PPCN vs. 27 °C for PPCN) (*SI Appendix*, Figs. S5 and S6). The LCST of the peptide-macromolecule conjugate allows the material to be applied as a liquid to the wound and transition to a gel due to the tissue's increased temperature (Fig. 3C). This property also allows gentle removal of the hydrogel by rinsing the wound with cooled saline during dressing changes, reducing additional trauma to regenerating tissue.

Oxidative stress has been shown to exacerbate inflammation and delay the healing of diabetic foot ulcers (23). Therefore, we

Fig. 1. All amino acid residues in the original sequence are required for A5G81 bioactivity. (A) HDF and HEKa were cultured on SAMs presenting a peptide (1 mol%) against a background of tri(ethylene glycol). Monolayers were prepared by immobilizing cysteine-terminated peptides onto maleimide-terminated dioctadecyl disulfide. (B) Adhesion of HDF and HEKa on SAMs presenting truncated versions of A5G81. (C) Adhesion of HDF and HEKa on SAMs presenting alanine-substituted versions of A5G81 (n = 3; all data are presented as mean ± SD).
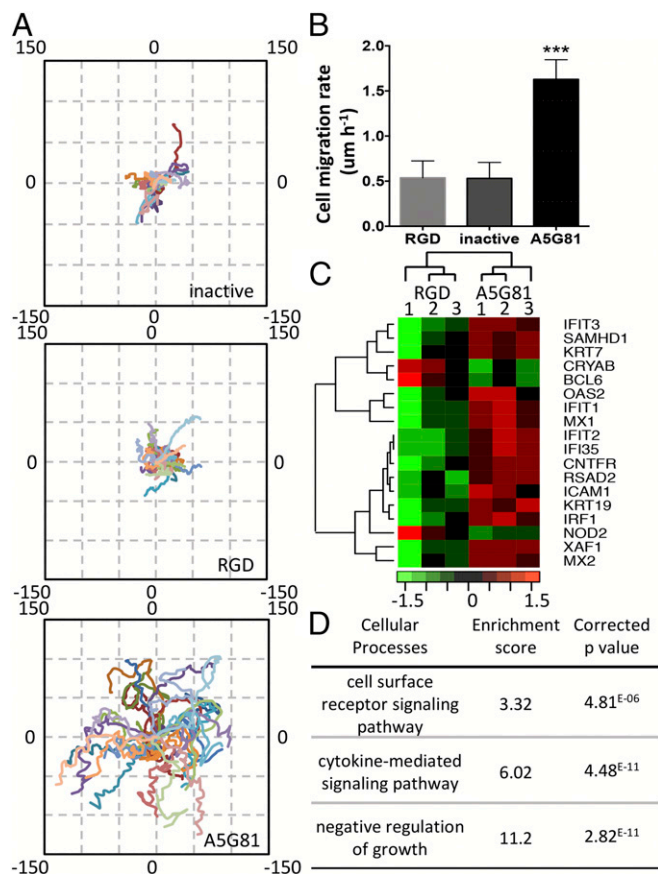
Fig. 2. A5G81 immobilized on 2D SAM surfaces promotes HEKa migration via haptokinesis. (*A*) The trajectories of 30 cells on inactive-, RGD-, and A5G81-presenting surfaces (all at 1 mol% peptide) were plotted in one field, oriented so that the cell's original location is $x(0)$, $y(0)$. The axes denote the migration distance in microns. (*B*) Mean rate of cell migration. All data are presented as mean ± SD; statistical significance was performed using one-way ANOVA with a Turkey's multiple comparison test ($n = 30$; ***$P < 0.001$). (*C*) Transcriptional profiling of HEKa cultured on A5G81 and RGD SAM surfaces (same molar concentration). The heat map of the top differentially expressed genes at the end of a 12-h culture period is shown. (*D*) The clusters of GO processes impacted by culturing the cells on the peptide-presenting SAM surfaces for 12 h.

and displayed fibroblast morphology. In contrast, cells entrapped in PPCN or inactive-PPCN remained rounded, suggesting minimal interactions with the matrix (Fig. 4*A*).

These findings confirm that the observed cell−matrix interactions are facilitated through specific ligand−receptor interactions between the cells and the tethered A5G81 and RGD peptides. It is significant that we observed an increased density of cells entrapped in the A5G81-PPCN hydrogels. Cell cycle analysis of cells entrapped in the various matrices at day 5 showed that a higher percentage of cells in A5G81-PPCN are in the DNA synthesis phase (Fig. 4*B* and *SI Appendix*, Table S1). This enhanced DNA synthesis activity within the cell population continued to increase from 21% at day 5 to 27% at day 10. A similar pattern was also observed in the RGD-PPCN group, with an increase from 13% at day 5 to 21% at day 10. The proliferation activity of cells entrapped in PPCN or inactive-PPCN was significantly lower than those measured in A5G81-PPCN and RGD-PPCN (Fig. 4*B*). Consistently, the total DNA quantification results show that A5G81-PPCN supported a higher cell proliferation rate over the course of 10 d than the other groups, confirming that A5G81 is able to promote the proliferation of HDFs in 3D (Fig. 4*C*). To further understand the mechanism for the enhanced proliferation of HDFs in A5G81-PPCN, we investigated the binding interactions between tethered A5G81 and the integrin receptors α3β1 and α6β1, which we confirmed are expressed by the cells using anti-α3 and anti-α6 antibodies (Fig. 4 *D* and *E*). Blocking only α3 or α6 leads to a partial decrease in cell proliferation, whereas blocking both α3 and α6 reduced cell proliferation to values that were comparable to those observed in the other hydrogels. Antibody blocking did not have an impact on cell proliferation in PPCN, inactive-PPCN, and RGD-PPCN. These results suggest that the increased cell proliferation within
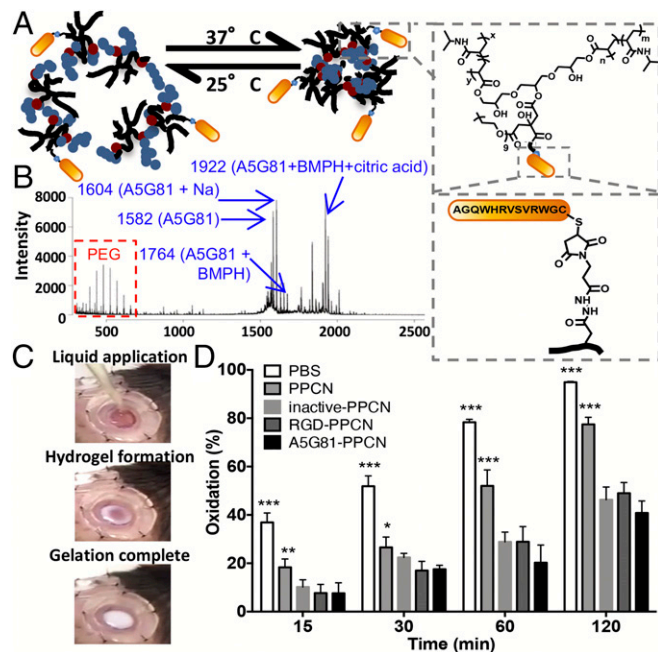
assessed whether the intrinsic antioxidant properties of PPCN were affected by the tethering of A5G81. The results of a lipid peroxidation inhibition assay show that conjugation of the peptides to PPCN resulted in protection against oxidation that was 125% and 160% that of PPCN's for RGD-PPCN and A5G81-PPCN, respectively (Fig. 3*D*). Further study of the intact peptides revealed that this enhanced antioxidant property of the peptide-functionalized PPCN is likely due to the intrinsic antioxidant property of the peptide itself (*SI Appendix,* Fig. S7), as certain amino acids are known to have antioxidant activities due to the reactivity of their side chains (24). Therefore, the thermoresponsive and antioxidant properties of PPCN, in combination with the properties of the tethered laminin-derived peptide A5G81, are expected to provide an optimal microenvironment that promotes tissue regeneration.

All of the hydrogel formulations supported the long-term viability of human dermal fibroblasts (HDFs) (Fig. 4*A*). Given that a scaffold for wound healing should facilitate the spreading, migration, and proliferation of surrounding cells into the scaffold, we used cytoplasmic calcein staining, confocal microscopy, and flow cytometry to evaluate cell spreading and proliferation of HDFs within the hydrogels. HDFs seeded in A5G81-PPCN and RGD-PPCN began to spread and interact with the surrounding matrix at day 5 postseeding, and, by day 10, cells were fully elongated

Fig. 3. Click chemistry enables the facile synthesis of thermoresponsive, antioxidant peptide-PPCN. (*A*) Schematic illustrating A5G81-PPCN self-assembly due to temperature change (*Left*). A5G81 peptide conjugation to PPCN via the cross-linker BMPH (*Right*). The same amount of peptide was conjugated across different peptide groups. (*B*) MALDI-TOF spectrum of A5G81-PPCN confirming the presence of the PPCN, peptide, peptide-linker, and peptide-linker-citric acid constructs. (*C*) A5G81-PPCN is applied as a liquid that covers the wound bed and conforms to the wound edges before gelation, due to body temperature, within seconds. (*D*) The β-carotene lipid peroxidation inhibition assay shows improved antioxidant activity of the peptide-modified PPCN ($n = 9$) (*$P < 0.05$; **$P < 0.01$; ***$P < 0.001$).
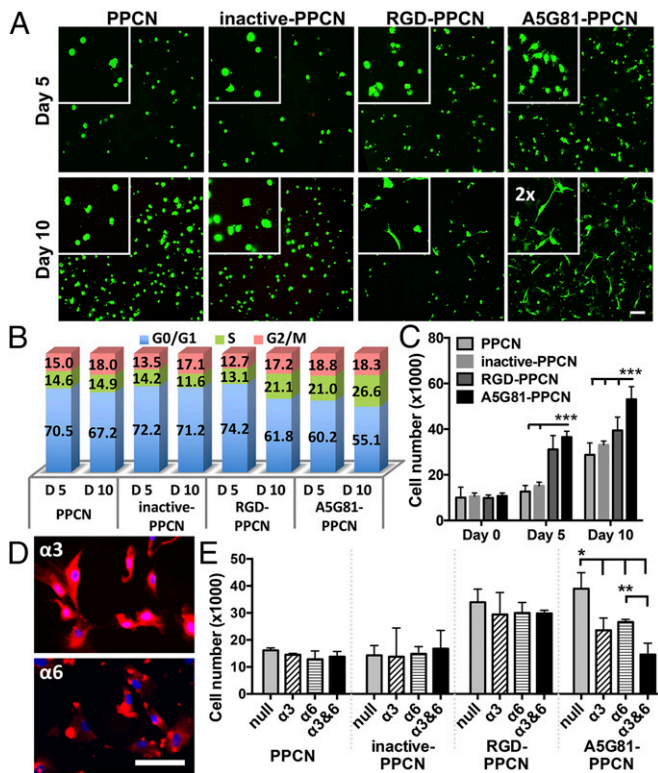
     Zhu et al.

Fig. 4. A5G81-PPCN promotes cell spreading and α3- and α6-mediated proliferation of entrapped HDF. (A) HDF entrapped within hydrogels and stained with Calcein-AM (live cells, green) and ethidium homodimer 1 (dead cells, red) at 5 and 10 d. (Scale bar: 100 μm.) Insets show a 2× magnified view of cell spreading. (B) Cell cycle analysis of the HDF in the hydrogels. (C) Cell proliferation within the hydrogel. (D) Staining of the integrin subunits α3 and α6 in HDF. (Scale bar: 100 μm.) (E) HDF proliferation response due to blocking integrin subunits α3 and/or α6. All data are presented as mean ± SD ($n \geq 5$; $*P < 0.05$; $**P < 0.01$; $***P < 0.001$).

A5G81-PPCN is mediated by the specific integrin-peptide interactions between the HDFs and tethered A5G81.

A5G81-PPCN Significantly Enhances Closure Rate, Reepithelialization, and Granulation Tissue Formation in Wounds of Diabetic Animals. We hypothesized that the observed enhanced in vitro cell proliferation and migration effects in A5G81-PPCN will translate to an accelerated wound healing response in vivo. To test this hypothesis, we investigated wound closure in a splinted excisional wound diabetic mouse model (25). This preclinical animal model is widely accepted as a first step to study wound healing therapies that could potentially benefit diabetic patients. All animals received two splinted dorsal wounds. One wound was treated with A5G81-PPCN, and the contralateral wound was treated with either RGD-PPCN, inactive-PPCN, or PPCN. Wounds treated with A5G81-PPCN healed at a significantly faster rate than wounds treated with the PPCN, inactive-PPCN, and RGD-PPCN, with 45% closure achieved at day 10 relative to 20% for inactive-PPCN and PPCN, and 31% for RGD-PPCN (Fig. 5 A–C). A5G81-PPCN also achieved 79% healing by day 15 and complete closure by day 22 postwounding (Fig. 5D and SI Appendix, Fig. S9).

Wound reepithelialization and granulation tissue formation was assessed histologically through measurements of the epithelial gap and granulation tissue thickness (Fig. 6 A–C and SI Appendix, Fig. S10). Histology of the regenerated wounded tissue at day 30 revealed close to complete reepithelialization in A5G81-PPCN–treated wounds, whereas PPCN-, inactive-PPCN–, and RGD-PPCN–treated wounds had remaining gaps of 2.15 ± 0.82 mm, 2.85 ± 1.08 mm, and 0.74 ± 0.64 mm, respectively (Fig.

6C and SI Appendix, Fig. S9). A5G81-PPCN–treated wounds had a multilayered epithelium structure that closely resembled healthy epidermis of the intact skin (26). The epithelial layer was significantly thinner in the RGD-PPCN–treated wounds, and discontinuities were observed in wounds treated with PPCN and inactive-PPCN (Fig. 6D and SI Appendix, Fig. S10B). A5G81-PPCN–treated wounds were also populated by a significant amount of α3 positive cells, which further supports the role of A5G81 in promoting cell infiltration and proliferation during the healing process (Fig. 6D). Staining for the macrophage cell marker F4/80 shows few macrophages in all groups, with the least amount within the A5G81-PPCN–treated tissue, suggesting a more subdued inflammatory status consistent with a more advanced stage of the healing process (Fig. 6D). To assess whether a significant difference in reepithelialization was also observed at an earlier time point, the wounded tissue of animals that received A5G81-PPCN and inactive-PPCN was assessed via histology at day 10 postwounding (SI Appendix, Fig. S11 A–C). Wounds treated with A5G81-PPCN have an average gap size of 0.4 ± 0.3 mm compared with 2.4 ± 0.6 mm for the wounds treated with inactive-PPCN ($P < 0.001$; SI Appendix, Fig. S11C). All wounds treated with A5G81-PPCN had granulation tissue that was more prominent relative to the contralateral wound (Fig. 6B and SI Appendix, Fig. S11C).

To benchmark A5G81-PPCN against another clinically used wound dressing for diabetic wound care management, we performed a side-by-side comparison study where one wound was treated with A5G81-PPCN and the contralateral wound was treated with the Promogran Prisma wound dressing (Systagenix), which is based on collagen and cellulose impregnated with silver. A5G81-PPCN outperformed Prisma starting on day 6 postwounding, with 50% of the wound area closed by day 15 and 90% closed by day 25. In contrast, wounds treated with Prisma exhibited 10% and 75% wound closure by days 15 and 25 postwounding, respectively (SI Appendix, Fig. S12 A–C). To mimic the presence of fluid in the wound, a condition often found in human wounds and not murine models, additional experiments
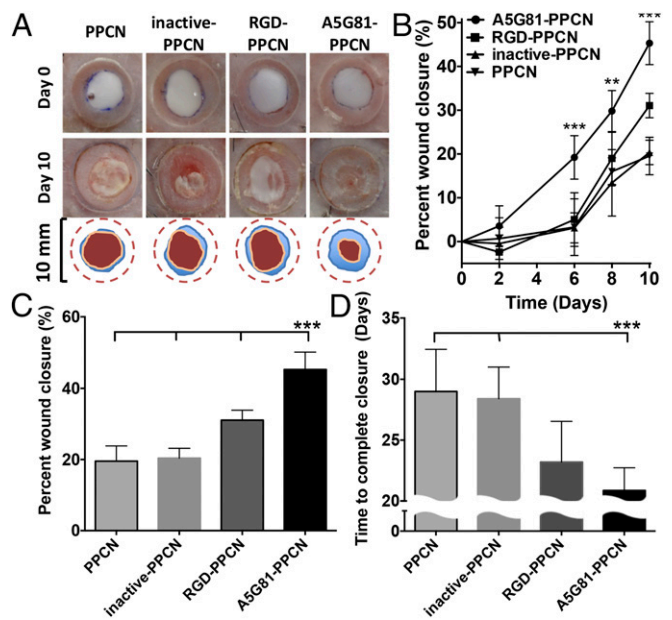

Fig. 5. A5G81-PPCN promotes accelerated regenerative wound closure of excisional splinted wounds in diabetic mice. (A) Representative images of the wound area immediately after wounding and at day 10 postwounding (Top, Middle). The wound-closure boundary at day 0 and day 10 postwounding is overlaid on the image (Bottom). (B) Wound healing 10 d postwounding. (C) Quantification of wound closure at day 10 postwounding for all four groups. (D) Summary of the complete wound-closure times. All data are presented as mean ± SD ($n \geq 5$; $***P < 0.01$).

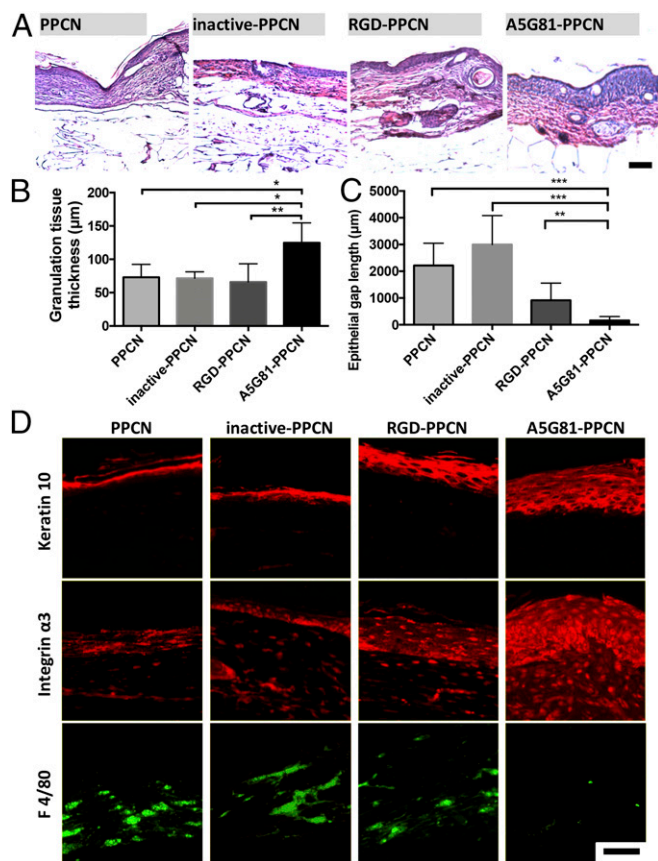MEDICAL SCIENCES

Fig. 6. A5G81-PPCN accelerates tissue regeneration in vivo. (*A*) H&E staining of tissue sections shows complete resorption of the hydrogel in all four groups 30 d postwounding. (*B*) Thicker granulation tissue was found in the A5G81-PPCN–treated wounds. (*C*) Quantification of the epithelial gap demonstrates that wounds treated with A5G81-PPCN exhibited the smallest epithelial gap and maximum wound closure. (*D*) Immunofluorescence staining of the wound, demonstrating enhanced expression of keratin-10, integrin α3, and reduced positive staining for macrophages (F4/80) in the A5G81-PPCN–treated wounds. (Scale bar: 100 μm.) All data are presented as mean ± SD ($n \geq 5$; *$P < 0.05$; **$P < 0.01$; ***$P < 0.001$).

were conducted with preswollen wet Prisma. A5G81-PPCN also outperformed the wet Prisma matrix (*SI Appendix,* Fig. S12 *D–F*).

Discussion

In order for chronic diabetic wounds to heal, skin cells must migrate and proliferate in a harsh microenvironment. We demonstrate that A5G81 is a potent adhesion ligand that is capable of facilitating both of these processes in an integrin-dependent manner that mimics laminin (11, 13). We also show that A5G81 covalently linked to a thermoresponsive antioxidant macromolecule is able to accelerate healing in splinted excisional wounds in diabetic mice. This animal model of hyperglycemia results in the characteristic diabetic complications observed in diabetic wound healing, including reduced chemokine and growth factor release, impaired angiogenesis, prolonged inflammation, and increased oxidative stress (25, 27). Another advantage of this model is the capability to mimic human wound healing processes by using a splint around the wound to prevent wound contraction, which is characteristic of wound healing in rodents, as they are loose-skin animals (28, 29). Therefore, the wound is allowed to heal mostly through tissue regeneration, resembling the healing process of humans (*SI Appendix,* Fig. S8) (30). Although various peptides have been successfully used to enhance wound healing in diabetic mice, most of these treatments involve topical application as a solution, requiring multiple repeat applications

(31–33). Furthermore, a majority of those studies also did not take into account skin contraction during the healing process. Therefore, it is unclear how treatments evaluated in rodent nonsplinted wound healing models affect the regeneration component of the healing process, which is the relevant process to wound healing in humans (31). For example, Van Slyke et al. (34) reported 70% closure in nonsplinted wounds within 7 d postwounding with the use of a soluble peptide derived from angiopoietin. There was no control of or accounting for how the treatment affects skin contraction, making it difficult to assess the potential benefit of their peptide for treating human wounds. Xiao et al. (35) recently reported the use of a tethered angiopoietin-derived peptide to heal nonsplinted wounds in diabetic mice and reported a 60% wound closure at day 14 with low-peptide treatment and 75% with high-peptide treatment. The peptide was tethered to a chitosan/collagen gel and added to the wound. Their histology data at days 14 and 21 postwounding show both contraction and regeneration as mechanisms for wound closure. The granulation tissue, as per their histology data, was also significantly less developed than what we observed in our study, reinforcing the importance of extracellular matrix proteins in promoting physiological wound healing. As for laminin-derived peptides, several dermal wound healing studies have reported that these peptides can play a positive role in accelerating wound closure (12, 33). Reported mechanisms include the promotion of angiogenesis and the support of keratinocyte migration (33, 36, 37). A brief summary of dermal wound healing studies that used laminin-derived peptides is included in *SI Appendix* to provide additional context to our findings (*SI Appendix,* Table S2). To our knowledge, A5G81 is the only laminin-derived peptide to date that exhibits a potent and synergistic effect on migration and proliferation for both keratinocytes and dermal fibroblasts. Furthermore, at the same molar concentration of tethered peptide, the effects of A5G81 were superior to those of RGD, a peptide commonly used to promote cell adhesion.

The accelerated wound healing observed in wounds treated with A5G81-PPCN compares favorably to wound-closure rates reported in this mouse model using growth factors and stem cell strategies. We previously reported 75% wound closure at day 15 and complete closure at 24 d postwounding when splinted wounds were treated with the slow release of low-dose stromal cell-derived factor 1α (38). Galiano et al. (39) reported an accelerated healing time of 17 d with the high dose of topical application of vascular endothelial growth factor. Two other research groups that investigated the treatment of wounds with allogeneic mesenchymal stem cells reported wound closures of 45% and 56% at day 15 and complete closure at 28 d postwounding (40, 41). Although promising, therapies that use cells, the local release of drugs, or the local release of macromolecules to promote wound healing will face higher regulatory challenges due to safety concerns, extended product development times, and higher costs.

Hydrogel dressings composed exclusively of peptides or extracellular matrix fragments have also shown promising results in treating dermal wounds in diabetic mice and can have an easier path to market (42, 43). However, the reported hydrogels do not have the shape-conforming and intrinsic antioxidant properties exhibited by the peptide-PPCN scaffold reported herein. Xiao et al. (35) and others have demonstrated that inhibiting oxidative stress in the wound can improve the wound healing response. Therefore, we probed healed wounds for markers of oxidative DNA damage. Wounds treated with A5G81-PPCN had significant attenuation of DNA oxidative damage relative to all other treatments (*SI Appendix,* Fig. S13). The decreased oxidative tissue damage may be due to the higher antioxidant nature of A5G81-PPCN or to a more advanced stage of healing in A5G81-PPCN–treated wounds. Therefore, this biomaterial-based approach to treat wound healing in diabetes may work through the simultaneous positive impact on the adhesion, proliferation, migration, and oxidative stress status of dermal cells. The strongest evidence for the treatment of diabetic ulcers using peptide hydrogels comes from a clinical trial using Argidene Gel—a peptide hydrogel matrix composed of RGD and sodium hyaluronate (44). The use of the RGD

hydrogel resulted in 4 times the number of patients with complete wound healing compared with the placebo group (44). Based on our results, we expect that the A5G81-PPCN dressing will provide a greater benefit to the patient.

Conclusion

We have identified and characterized a laminin-derived peptide with unique receptor-mediated and antioxidant properties that are beneficial to the wound healing process. Conjugating this peptide to PPCN resulted in a shape-conforming material that can be used as a regenerative dressing to enhance wound healing. Notably, A5G81 outperformed the fibronectin-derived cell adhesion peptide RGD in its ability to induce cell motility and proliferation in vitro, and the mechanism was shown to involve the integrin subunits $\alpha3$ and $\alpha6$. Future studies will investigate A5G81-PPCN in a large animal model for wound healing.

Materials and Methods

Peptide Conjugation and Characterization. Conjugation was achieved using the bifunctional linker N-β-maleimidopropionic acid hydrazide (BMPH) (Thermo Fisher) The completion of the reaction between the peptide and the BMPH-PPCN was confirmed by quantifying free thiol groups in the reaction medium over time using Ellman's reagent. The successful conjugation was confirmed using MALDI-TOF (Fig. 3B and SI Appendix, Fig. S3). The generation of primary amines within PPCN due to the conjugation was quantified with the trinitrobenzenesulfonic assay and used to calculate the final concentration of peptide tethered to PPCN using a standard curve for each peptide. The 1 mol% peptide on all SAM surfaces was verified by the peak intensity ratio between the peptide-maleimide-PEG-alkanethiols and the PEG-end-capped alkanethiols via MALDI-TOF mass spectrometry (18).

Diabetic Wound Healing Model. All the experimental procedures involving animals were approved by the Institutional Animal Care and Use Committee of Northwestern University. The in vivo performance of the hydrogels was evaluated using a splinted excisional wound model in type II diabetic mice [B6.BKS(D)-Lepr^db/J; The Jackson Laboratory] as previously described (25, 38). Doughnut-shaped acrylate splints were attached to the left and right dorsal sides of the mouse, and a 6-mm circular, full-thickness wound was made in the center of each splinted area. Forty microliters of PPCN solution was applied to each wound bed and covered with TegaDerm.

Statistical Analysis. GraphPad Prism 6.0c was used for two-way ANOVA tests to measure differences for experiments with multiple data sets. A Tukey test was performed between groups with significant differences to correct for the multiple pair-wise comparisons. A value of $P \leq 0.05$ was considered to be statistically significant.

Details for the materials and methods used for our protocols are provided in SI Appendix.

1. Centers for Disease Control and Prevention (2014) National Diabetes Statistics Report: Estimates of diabetes and its burden in the United States (Centers Dis Control Prevention, Atlanta).
2. World Health Organization (2016) Global Report on Diabetes (World Health Org, Geneva).
3. Falanga V (2005) Wound healing and its impairment in the diabetic foot. Lancet 366: 1736–1743.
4. Smiell JM, et al. (1999) Efficacy and safety of becaplermin (recombinant human platelet-derived growth factor-BB) in patients with nonhealing, lower extremity diabetic ulcers: A combined analysis of four randomized studies. Wound Repair Regen 7:335–346.
5. Hu S, Kirsner RS, Falanga V, Phillips T, Eaglstein WH (2006) Evaluation of Apligraf persistence and basement membrane restoration in donor site wounds: A pilot study. Wound Repair Regen 14:427–433.
6. Zheng D, et al. (2012) Topical delivery of siRNA-based spherical nucleic acid nanoparticle conjugates for gene regulation. Proc Natl Acad Sci USA 109:11975–11980.
7. Schäfer M, Werner S (2008) Cancer as an overhealing wound: An old hypothesis revisited. Nat Rev Mol Cell Biol 9:628–638.
8. Ziyadeh N, Fife D, Walker AM, Wilkinson GS, Seeger JD (2011) A matched cohort study of the risk of cancer in users of becaplermin. Adv Skin Wound Care 24:31–39.
9. Seet WT, et al. (2012) Shelf-life evaluation of bilayered human skin equivalent, MyDerm™. PLoS One 7:e40978.
10. Lamme EN, van Leeuwen RT, Mekkes JR, Middelkoop E (2002) Allogeneic fibroblasts in dermal substitutes induce inflammation and scar formation. Wound Repair Regen 10:152–160.
11. Goldfinger LE, et al. (1999) The α3 laminin subunit, α6β4 and α3β1 integrin coordinately regulate wound healing in cultured epithelial cells and in the skin. J Cell Sci 112:2615–2629.
12. Rousselle P, et al. (April 9, 2013) The syndecan binding sequence KKLRIKSKEK in laminin α3 LG4 domain promotes epidermal repair. Eur J Dermatol, 10.1684/ejd.2013.1974.
13. Frank DE, Carter WG (2004) Laminin 5 deposition regulates keratinocyte polarization and persistent migration. J Cell Sci 117:1351–1363.
14. Nielsen PK, et al. (2000) Identification of a major heparin and cell binding site in the LG4 module of the laminin α 5 chain. J Biol Chem 275:14517–14523.
15. Katagiri F, et al. (2012) Screening of integrin-binding peptides from the laminin α4 and α5 chain G domain peptide library. Arch Biochem Biophys 521:32–42.
16. Humphries JD, Byron A, Humphries MJ (2006) Integrin ligands at a glance. J Cell Sci 119:3901–3903.
17. Yang J, van Lith R, Baler K, Hoshi RA, Ameer GA (2014) A thermoresponsive biodegradable polymer with intrinsic antioxidant properties. Biomacromolecules 15:3942–3952.
18. Mrksich M (2009) Using self-assembled monolayers to model the extracellular matrix. Acta Biomater 5:832–841.
19. Sobers CJ, Wood SE, Mrksich M (2015) A gene expression-based comparison of cell adhesion to extracellular matrix and RGD-terminated monolayers. Biomaterials 52:385–394.
20. Eden E, Navon R, Steinfeld I, Lipson D, Yakhini Z (2009) GOrilla: A tool for discovery and visualization of enriched GO terms in ranked gene lists. BMC Bioinformatics 10:48.
21. García-Conesa MT, Tribolo S, Guyot S, Tomás-Barberán FA, Kroon PA (2009) Oligomeric procyanidins inhibit cell migration and modulate the expression of migration and proliferation associated genes in human umbilical vascular endothelial cells. Mol Nutr Food Res 53:266–276.
22. Vejlsgaard GL, et al. (1989) Kinetics and characterization of intercellular adhesion molecule-1 (ICAM-1) expression on keratinocytes in various inflammatory skin lesions and malignant cutaneous lymphomas. J Am Acad Dermatol 20:782–790.
23. Schäfer M, Werner S (2008) Oxidative stress in normal and impaired wound repair. Pharmacol Res 58:165–171.
24. Meucci E, Mele MC (1997) Amino acids and plasma antioxidant capacity. Amino Acids 12:373–377.
25. Michaels J, 5th, et al. (2007) db/db mice exhibit severe wound-healing impairments compared with other murine diabetic strains in a silicone-splinted excisional wound model. Wound Repair Regen 15:665–670.
26. Brem H, Tomic-Canic M (2007) Cellular and molecular basis of wound healing in diabetes. J Clin Invest 117:1219–1222.
27. Werner S, Breeden M, Hübner G, Greenhalgh DG, Longaker MT (1994) Induction of keratinocyte growth factor expression is reduced and delayed during wound healing in the genetically diabetic mouse. J Invest Dermatol 103:469–473.
28. Galiano RD, Michaels J, 5th, Dobryansky M, Levine JP, Gurtner GC (2004) Quantitative and reproducible murine model of excisional wound healing. Wound Repair Regen 12:485–492.
29. Greenhalgh DG (2003) Wound healing and diabetes mellitus. Clin Plast Surg 30:37–45.
30. Park SA, et al. (2015) Importance of defining experimental conditions in a mouse excisional wound model. Wound Repair Regen 23:251–261.
31. Livant DL, et al. (2000) The PHSRN sequence induces extracellular matrix invasion and accelerates wound healing in obese diabetic mice. J Clin Invest 105:1537–1545.
32. Rodgers KE, et al. (2003) Histological evaluation of the effects of angiotensin peptides on wound repair in diabetic mice. Exp Dermatol 12:784–790.
33. Iorio V, Troughton LD, Hamill KJ (2015) Laminins: Roles and utility in wound repair. Adv Wound Care (New Rochelle) 4:250–263.
34. Van Slyke P, et al. (2009) Acceleration of diabetic wound healing by an angiopoietin peptide mimetic. Tissue Eng Part A 15:1269–1280.
35. Xiao Y, et al. (2016) Diabetic wound regeneration using peptide-modified hydrogels to target re-epithelialization. Proc Natl Acad Sci USA 113:E5792–E5801.
36. Malinda KM, Wysocki AB, Koblinski JE, Kleinman HK, Ponce ML (2008) Angiogenic laminin-derived peptides stimulate wound healing. Int J Biochem Cell Biol 40: 2771–2780.
37. Min SK, et al. (2010) The effect of a laminin-5-derived peptide coated onto chitin microfibers on re-epithelialization in early-stage wound healing. Biomaterials 31: 4725–4730.
38. Zhu Y, et al. (2016) Sustained release of stromal cell derived factor-1 from an antioxidant thermoresponsive hydrogel enhances dermal wound healing in diabetes. J Control Release 238:114–122.
39. Galiano RD, et al. (2004) Topical vascular endothelial growth factor accelerates diabetic wound healing through increased angiogenesis and by mobilizing and recruiting bone marrow-derived cells. Am J Pathol 164:1935–1947.
40. Shin L, Peterson DA (2013) Human mesenchymal stem cell grafts enhance normal and impaired wound healing by recruiting existing endogenous tissue stem/progenitor cells. Stem Cells Transl Med 2:33–42.
41. Wu Y, Chen L, Scott PG, Tredget EE (2007) Mesenchymal stem cells enhance wound healing through differentiation and angiogenesis. Stem Cells 25:2648–2659.
42. Philp D, et al. (2003) Thymosin beta 4 and a synthetic peptide containing its actin-binding domain promote dermal wound repair in db/db diabetic mice and in aged mice. Wound Repair Regen 11:19–24.
43. Roy DC, Mooney NA, Raeman CH, Dalecki D, Hocking DC (2013) Fibronectin matrix mimetics promote full-thickness wound repair in diabetic mice. Tissue Eng Part A 19: 2517–2526.
44. Steed DL, et al.; RGD Study Group (1995) Promotion and acceleration of diabetic ulcer healing by arginine-glycine-aspartic acid (RGD) peptide matrix. Diabetes Care 18: 39–46.

MEDICAL SCIENCES